Vaccine 37 (2019) 6380–6389

Contents lists available at ScienceDirect

Vaccine

journal homepage: www.elsevier.com/locate/vaccine

A scale-down model of 4000-L cell culture process for inactivated foot-and-mouth disease vaccine production

Xin-Ran Li [a,b,1], Yan-Kun Yang [a,b,c,1], Rong-Bin Wang [c,d], Fang-Lan An [e], Yun-De Zhang [e], Jian-Qi Nie [a,b], Hadji Ahamada [c,d], Xiu-Xia Liu [b,d], Chun-Li Liu [b,d], Yu Deng [b,d], Zhong-Hu Bai [b,c,d,*], Ye Li [b,*], Xue-Rong Liu [e,*]

[a] The Key Laboratory of Industrial Biotechnology, Ministry of Education, School of Biotechnology, Jiangnan University, Wuxi 214122, China
[b] National Engineering Laboratory for Cereal Fermentation Technology, Jiangnan University, Wuxi 214122, China
[c] The Key Laboratory of Carbohydrate Chemistry and Biotechnology, Ministry of Education, School of Biotechnology, Jiangnan University, Wuxi 214122, China
[d] Jiangsu Provincial Research Center for Bioactive Product Processing Technology, Jiangnan University, Wuxi 214122, China
[e] China Agricultural Veterinary Biological Science and Technology Co., Ltd, Lanzhou 730046, China

ARTICLE INFO

Article history:
Received 1 May 2019
Received in revised form 1 September 2019
Accepted 4 September 2019
Available online 10 September 2019

Keywords:
Scale-down model
FMD vaccine
Cell culture
CFD simulation
QbD

ABSTRACT

The anticipated increasing demand for inactivated foot-and-mouth (FMD) disease vaccine calls for its larger production capacity, while development of a large-scale process typically requires high running cost and has very limited experimental throughput at manufacturing scale. Thus, an economic scale-down model of representing a large-scale process becomes necessary and essential. In this study, we used a systematic approach to establish a scale-down model representing a 4000-L culture process for FMD vaccine production by suspension BHK-21 cells. In detail, we firstly compared hydrodynamic properties of three bioreactors (14-L, 800-L and 4000-L) under three different conditions (equivalent mixing time, equivalent shear stress and equivalent volumetric power). We figured out equivalent volumetric power (P/V) potentially as an appropriate scale-down strategy, since it resulted in comparable calculated hydrodynamic parameters among three bioreactors. Next, we used computational fluid dynamics (CFD) simulation to provide more details about hydrodynamic environments inside the bioreactors, which supports the reliability of this scale-down strategy. Finally, we compared cell growth, metabolites, vaccine productivity and product quality attributes during FMD vaccine production by BHK-21 cells and observed very close performances among three bioreactors, which once again demonstrates the robustness of this scale-down model. This scale-down strategy can be applied to study variations and critical quality attributes (CQAs) in the resultant production process based on quality by design (QbD) principles, aiming at further more efficient optimization of vaccine production.

1. Introduction

Foot-and-mouth disease (FMD), which has threatened countless lives of more than 100 kinds of cloven-hoofed animal for centuries, was identified as the most dangerous animal disease by the World Organization for Animal Health (OIE) [1]. FMD is caused by foot-and-mouth disease virus (FMDV) [2,3], and inactivated vaccine is conceived as the most effective strategy for the prevention and control of FMD for its economic practicality and immune effect [4,5]. Invention of FMD inactivated vaccine has a history of nearly 100 years, which can be dated to 1925 [6]. Since the first continuous cell line was discovered in 1948 [7], a variety of cell lines (tongue epithelium, Madin-Darby bovine kidney cells [8] and baby hamster kidney) have been used to produce FMD vaccine. Baby hamster kidney (BHK) cell line soon became the dominant cell line for FMD inactivated vaccine production, due to its excellent performance in full suspension culture [9]. In 1962, BHK cell line was domesticated into freely suspended cells [10], and was cultured commercially in agitated, stainless steel bioreactors soon after that. Since then, production of FMD inactivated vaccine entered the stage of full suspension culture in stirred tank bioreactors.

Despite of these advances, quite a few issues still need to be addressed in regard to FMD inactivated vaccine production. For example, mammalian cells don't have cell wall and are prone to be damaged by turbulent fluid dynamic stress (particularly caused by agitation [11]), while impeller agitation is required to maintain

* Corresponding authors at: National Engineering Laboratory for Cereal Fermentation Technology, Jiangnan University, Wuxi 214122, China (Z.-H. Bai).
E-mail addresses: baizhonghu@jiangnan.edu.cn (Z.-H. Bai), yeli0622@jiangnan.edu.cn (Y. Li), lxr0931@126.com (X.-R. Liu).
[1] The co-first authors contributed equally to this work.

https://doi.org/10.1016/j.vaccine.2019.09.013
0264-410X/

homogeneity in a mixing tank. Such conflict must be resolved in order for further process optimization. What's more, complexity of the gas-solid-liquid system, unknown fluid properties at the end-flow area and unknown interactions between cells and environment, should also be systematically investigated and characterized. However, huge experimental cost at industrial scale for FMD inactivated vaccine production makes comprehensive process optimization very challenging. A scale-down model representing the large-scale FMD inactivated vaccine process is thus desired, in order to study process optimization in an economic way. Actually, successes in scaling up imply that development of scale-down model is possible [12–15]. There were quite a few reports about development of scale-down models [16–19]. In general, in the development of a scale-down model, mixing time, volumetric mass transfer coefficient (k_La) [20], oxygen transfer rate (OTR), volumetric power (P/V) [21] and shear stress [22], are the common parameters selected as scale-down strategies, which strongly connect with the geometry of a fermentation tank. Meanwhile, a distributed-parameter model is preferred, which considers the actual hydrodynamics of a mixing tank. This requires accurate information about the flow field properties in the mixer, which nowadays can be obtained by computational fluid dynamics (CFD) simulation technology through applying conservation equations for mass, momentum and energy, together with additional sets of equations [23]. There were also several reports of using CFD simulation to study mixing tanks [24]. For example, Noorman used CFD simulation technology to study the gas, fluid and metabolic characteristics of fermentation by yeast in a 30-m^3 bioreactor [16]. Ahuja et al. used the method of multi-variate analysis and mass transfer to refine a 3-L bioreactor scale-down model from a 15,000-L bioreactor for monoclonal antibody production [17]. Delvigne et al. linked CFD, metabolic flux analysis and agent-based modelling (ABM) for better understanding of the cell lifelines in a heterogeneous environment [18]. Haringa et al. used hydrodynamic-metabolic modeling to establish a scale-down model by Euler-Lagrange CFD simulation [19].

In the previously study, we successfully established an empirical scale-up model for vaccine production, with both productivity and product quality reaching the releasing specification. However, further systematic optimization towards steady performance of the large-scale reactor is needed, since the product quality varied significantly from batch to batch (unpublished data). As the first step towards this comprehensive optimization in an economic way, we developed a scale-down model in this study. In detail, we firstly chose equivalent mixing time, equivalent shear stress and equivalent P/V as the scale-down candidates, and compared several calculated hydrodynamic parameters for 14-L, 800-L and 4000-L bioreactors, respectively. We figured out equivalent P/V was potentially an appropriate scale-down strategy within the range of hydrodynamic conditions mammalian cells can tolerant, since it resulted in comparable calculated hydrodynamic parameters among three bioreactors. Next, we used CFD simulation describe the details of hydrodynamics at constant P/V for different bioreactors, which conformed to calculated results in general. Meanwhile, we also adjusted volumetric oxygen mass transfer coefficient (k_La) by modifying aeration rates so that gas transfer was no longer a limiting factor in the established scale-down model. This equivalent P/V strategy was then applied in the production of FMD inactivated vaccine in 14-L, 800-L and 4000-L bioreactors. Similar behaviors of three bioreactors and quality attributes were observed, which demonstrated the reliability of the scale-down model developed in this study. Finally, we applied design of experiments (DOE) by using this model in accordance with QbD principle, which improved stability of product quality significantly at manufacture scale.

2. Materials and methods

2.1. Bioreactor configuration

To establish the FMD vaccine scale-down model, three different bioreactors systems (14-L, 800-L and 4000-L bioreactors) were tested in this study. Geometrical parameters of the bioreactors are listed in Table 1. Impellers of the bioreactors are depicted in Fig. 1a. Air was sparged from a single pipe for each bioreactor. It should be noted that the 800-L bioreactor has the impeller not at the central axis, which is different from the other two bioreactors (14-L and 4000-L) (Fig. 1b).

2.2. Cell culture process in bioreactors

BHK-21 suspension cell line adapted from BHK21C13-2P cell line (ECACC CRL-84111301) was used to produce FMD vaccine in modifying Minimum Essential Media (MD611, Merck, United States), supplemented with 4% (v/v) of newborn bovine serum (Runsun, China). Cells were initially inoculated and grown in 125-mL, 500-mL and 3-L shake flasks (Corning, New York, USA) at 37 °C for 48 h in humidified atmosphere containing 5% CO_2. Seeds were then transferred into three bioreactors with initial cell density of 0.5×10^6 viable cells/mL. During the cell culture process in three bioreactors, temperature was controlled at 36.5 °C. 10% w/v sodium bicarbonate and CO_2 gas were used to maintain pH at 7.2. Dissolved oxygen (DO) set-point was 65% through sparing of air and oxygen mixture. Samples were taken every 6 h to evaluate viable cell density, viability, metabolites and product quality, until 48 h.

2.3. Virus infection and FMD inactivated vaccine production

After BHK-21 cells were grown in bioreactors for 48 h, we replaced the culture media with fresh modified Minimum Essential Medium containing FMD virus (O/MYA98/BY/2010, China Agricultural Veterinarian Biology Science & Technology Co. Ltd., Lanzhou, Gansu Province, China) ($TCID_{50} = 10^{-7.50}$ virions/mL), with multiplicity of infection (MOI) = 0.01. In all three bioreactors for vaccine production, temperature was controlled at 36.5 °C. 10% w/v sodium bicarbonate and CO_2 gas were used to maintain pH between 7.4 and 7.6. The DO set-point was 65% through sparing of air and oxygen mixture. Sample were taken every 6 h for totally 12 h.

2.4. Calculation of hydrodynamic parameters

When Reynolds number >10^4, the fluid flow regime is turbulence. Mixing time (t_{mix}) is calculated by using Eqs. (1) and (2) [12]:

$$t_{mix} = K_1 V^{a_1} Re^{b_1} / D \quad (1)$$

$$Re = \rho N D^2 / \mu \quad (2)$$

Table 1
Geometric parameters of the 14-L, 800-L and 4000-L bioreactors used in this study.

	14-L	800-L	4000-L
Diameter (T, mm)	220	750	1400
Bottom Type	Dished	Dished	Dished
Filled volume (VL, L)	10	500	3000
Capacity (V, L)	14	800	4000
Baffle length (L, mm)	–	1130	1795
Baffle width (W, mm)	–	80	120
Impellers (D, mm)	120	320	480

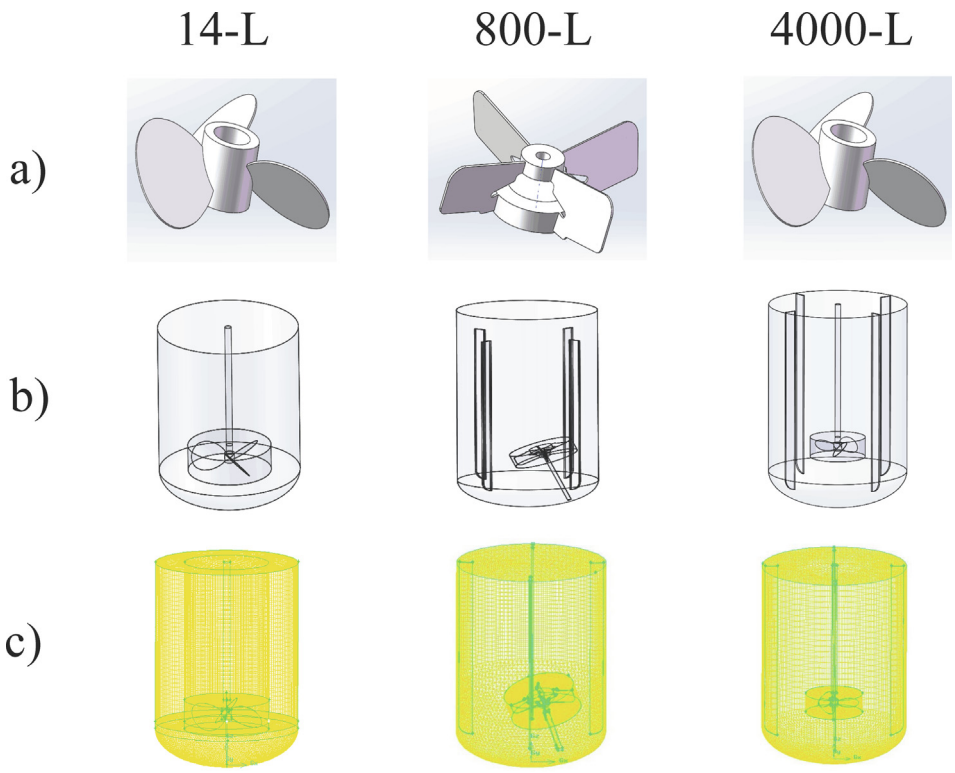

Fig. 1. Impeller shapes (a), reactor configurations (b) and computational grids used in simulation (c) for the three bioreactors used in this study.

where K_1, a_1 and b_1 are constants; V is liquid volume in the bioreactor (L); D is diameter of the impeller (m); Re is Reynolds number; ρ is broth density (kg/m^3); N is impeller agitation rate (s^{-1}) and μ is dynamic viscosity (Pa s).

Shear stress (τ^k) in a stirred bioreactor is calculated according to Kolmogorov turbulence flow theories by using Eqs. (3) and (4) [25]:

$$\tau^k = \rho(\varepsilon v)^{1/2} \tag{3}$$

$$\varepsilon = \frac{nN_pN^3D^5}{V} \tag{4}$$

where ε is local energy dissipation rate of turbulent flow (W/kg); $\varepsilon = (P/V)/\rho$; n is number of impellers; N_p is power number; v is kinematic viscosity (m^2/s); $v = \mu/\rho$. When $V = V_1(V_i = D^3)$, the shear stress represents local shear stress near the impeller.

Likewise, according to Kolmogorov turbulence flow theories, the eddy size is calculated by the Eq. (5) [25]:

$$\eta = (v^3/\varepsilon)^{1/4} \tag{5}$$

The impeller tip speed is calculated using the following Eq. (6):

$$U_T = \pi ND \tag{6}$$

Based on the power number (Np) of the impeller, P/V is calculated using the Eq. (7) [26]:

$$P/V = N_p\rho N^3D^5/V \tag{7}$$

2.5. Numerical models used in CFD simulation

The continuity equation representing conservation of mass is expressed as:

$$\frac{\partial(u)}{\partial x} + \frac{\partial(v)}{\partial y} + \frac{\partial(w)}{\partial z} = 0 \tag{8}$$

where u, v, w represent velocity component of x, y, z direction, respectively.

Momentum conservation equation in an inertial reference frame is described as:

$$\frac{\rho D(u_j)}{Dt} = -\frac{\partial p}{\partial x_j} + \mu\frac{\partial^2 u_j}{\partial x_i^2} + \rho f_j \tag{9}$$

where ρ is hydrodynamic density (kg/m^3); μ is average viscosity; p is pressure.

Energy conservation equation is described as:

$$\frac{\partial(\rho T)}{\partial t} + div(\rho uT) = div[\frac{k}{c_p}gradT] + S_T \tag{10}$$

where Cp is molar heat capacity at constant pressure; T is thermodynamic temperature; k is heat transfer coefficient of fluid, S_T is source term. Turbulent model is described by the following standard k–ε double equations [27]:

$$\frac{\partial(\rho k)}{\partial t} + \frac{\partial(\rho k u_i)}{\partial x_i} = \frac{\partial}{\partial x_j}\left[\left(\mu + \frac{\mu_t}{\sigma_k}\right)\frac{\partial k}{\partial x_j}\right] + G_k - \rho\varepsilon \tag{11}$$

$$\frac{\partial(\rho\varepsilon)}{\partial t} + \frac{\partial(\rho\varepsilon u_i)}{\partial x_i} = \frac{\partial}{\partial x_j}\left[\left(\mu + \frac{\mu_t}{\sigma_\varepsilon}\right)\frac{\partial\varepsilon}{\partial x_j}\right] + \frac{C_{1\varepsilon}\varepsilon}{k}G_k - C_{2\varepsilon\rho}\frac{\varepsilon^2}{k} \tag{12}$$

where μ_t is the turbulent viscosity; $C_{1\varepsilon}$ and $C_{2\varepsilon}$ represent model constants; σ_k and σ_ε are Prandtl numbers for turbulence energy k and dissipation rate ε, respectively. $C_{1\varepsilon} = 1.44$, $C_{2\varepsilon} = 1.92$, $\sigma_k = 1.0$, and $\sigma_\varepsilon = 1.3$.

2.6. CFD simulation

Commercial CFD software (Fluent, Inc., Fluent 14.5, Lebanon, New Hampshire, USA) was used to simulate the flow fields in 14-L, 800-L and 4000-L bioreactors. The simulation procedure includes the following steps:

1. Physical models were firstly constructed by solid Works 2014 (Dassault Systèmes, Concord, Massachusetts, USA) 3D design software, based on the geometrical parameters of each bioreactor in Table 1.
2. The entire luminal geometrical models were generated and meshed in a specialized preprocessing program (Fluent, Inc., GAMBIT 2.4.6, Lebanon, New Hampshire, USA). A mesh consisting primarily of tetrahedral finite elements was generated for the individual models. The grid was created by first grading the edges of the specified "source" faces with appropriate numbers of nodes, followed by generating the surface meshes using PAVE scheme. Next, the volume mesh was generated using the Cooper meshing scheme to sweep the mesh node patterns of specified "source" faces through the volume. To improve the accuracy of simulation, impeller area was dealt with by using unstructured grids, while other areas were dealt with by using structured grids.
3. Medium was selected as the simulation material, and fluid-dependent turbulence model was activated by setting k-ε turbulence model for liquid phase.
4. Stationary domain for the tank bulk and rotate domain for impeller swept zone by setting rotation speed were defined. Surface tension coefficient was selected and set. Inter phase force option was activated by setting drag force model and turbulence dissipation force model. Property boundary conditions were then set for the model. Shaft was set as rotating wall; sparger was set at the gas inlet, which is located near the bottom of the bioreactor.
5. Gravitational acceleration for considering the buoyancy effect was activated. Governing equations for mass, momentum, and phase balance were then solved using Fluent 14.5. The converged steady state solution of the simulation was assumed when all the variable residuals were less than 10^{-5}.

2.7. Volumetric oxygen mass transfer coefficient (k_La)

A dynamic technique described by Rao [28] was used to estimate the k_La at three different scales. Dynamic determination of k_La was based on supplying oxygen to a fluid that is depleted of oxygen by nitrogen sparging. Oxygen transfer rate is governed by the following equation.

$$\frac{d[o_2]}{dt} = k_La([o_2]^* - [o_2]) \quad (13)$$

The on-line dissolved oxygen (DO) reading was used to obtain $[O_2]$, which was plotted versus time to obtain a correlation from which $d[O_2]/dt$ was calculated. Next, $d[O_2]/dt$ was plotted versus $[O_2]$, and the slope is k_La. We assumed that the gas phase was well mixed and equal to the inlet air composition. This assumption also implies that $[O_2](t)$ was constant everywhere in the bioreactor and equal to the saturation concentration with respect to air. This allows for simple solutions of unsteady state equations to calculate k_La.

2.8. Analytical methods

Cell density and viability were assessed by an automated cell counting device (CASY Model TT, Innovatis AG, Reutlingen, Germany) with trypan blue staining method. Cell culture metabolites, such as glucose, glutamine, lactate, ammonia, and osmotic pressure were measured by the NOVA Bio-Profile 100 biochemical analyzer (Nova Biomedical Corporation, Waltham, MA, USA). Median tissue culture infectious dose ($TCID_{50}$) based on the cytopathic effect was measured according to a previous report [29]. 146 s antigen was measured using sucrose density gradient centrifugation [30]. Total protein concentrations were measured by modified Lowry assay described in ASTM D5712-10 (Standard Test Method for Analysis of Aqueous Extractable Protein in Natural Rubber and its Products Using the Modified Lowry Method).

2.9. PLS batches model

The data was modeled as described by Wold et al. [31], using the modeling setup denoted as Observation-Wise Unfolding with subsequent Batch-Wise Unfolding of the scores (OWU-BWU). SIMCA-P version 13 (Umetrics, Umea, Sweden) was used to build the PLS batches model.

3. Results

3.1. Physical models

Physical models of three different bioreactors were firstly constructed by Solid Works 3D design software. As shown in Fig. 1b, models were built up based on oars, baffles and geometry of bioreactors. The 3D grids were then generated by GAMBIT software according to the models. Three bioreactors were divided into 2.84×10^5, 3×10^5, 3.59×10^5 3D grids, with mass of each grid 0.89, 0.83, 0.86, respectively (Fig. 1c).

3.2. Mixing time

In order to certify a turbulence model for each bioreactor, the Reynolds number must exceed 1000. Hence, according to Eq. (2), the calculated agitation speeds should not be less than 42, 6 and 3 rpm for three bioreactors, respectively. We applied CFD and obtained mixing time with five agitation speeds. According to Eq. (1), the relationship of agitation speed and mixing time is established as:

$$14-\mathrm{L} \quad t_{mix} = 448N^{-0.70} \quad R^2 = 0.998 \quad (14)$$

$$800-\mathrm{L} \quad t_{mix} = 1002N^{-0.81} \quad R^2 = 0.987 \quad (15)$$

$$4000-\mathrm{L} \quad t_{mix} = 6948N^{-1.27} \quad R^2 = 0.974 \quad (16)$$

High correlation indexes (>0.97) suggests satisfactory regressions for all three bioreactors.

3.3. Identification of equivalent P/V as the scale-down strategy

For three bioreactors, we initially set equivalent mixing time, equivalent shear stress and equivalent P/V, and calculated the corresponding unknown hydrodynamic parameters for each case using equations described before (mixing time by Eqs. (14)–(16), P/V by Eq. (7), impeller tip speed by Eq. (6), shear stress Eq. (3) and eddy size by Eq. (5), respectively) (Fig. 2). In Case 1 when we set mixing time to 50 s, all parameters of three bioreactors are within the cell tolerant ranges [25,32]. However, P/V value in this case displays 20-fold variance between 14-L and 4000-L scales, which could lead to dramatically different microenvironment inside the bioreactors and hence dissimilar cell performances for vaccine production between the two bioreactors. In Case 2 when we set shear stress to 0.3 N/m^2, P/V value in 14-L bioreactor reaches 15.77 W/m^3, much higher than the values (<5 W/m^3) reported in other studies [33–35], which may result in cell damage and hence poor cell growth. In Case 3 when we set P/V value to 3 W/m^3, all hydrodynamic parameters are within acceptable and similar ranges for all three scales, which indicates constant P/V value is potentially a reliable scale-down strategy in our system for FMD vaccine production.

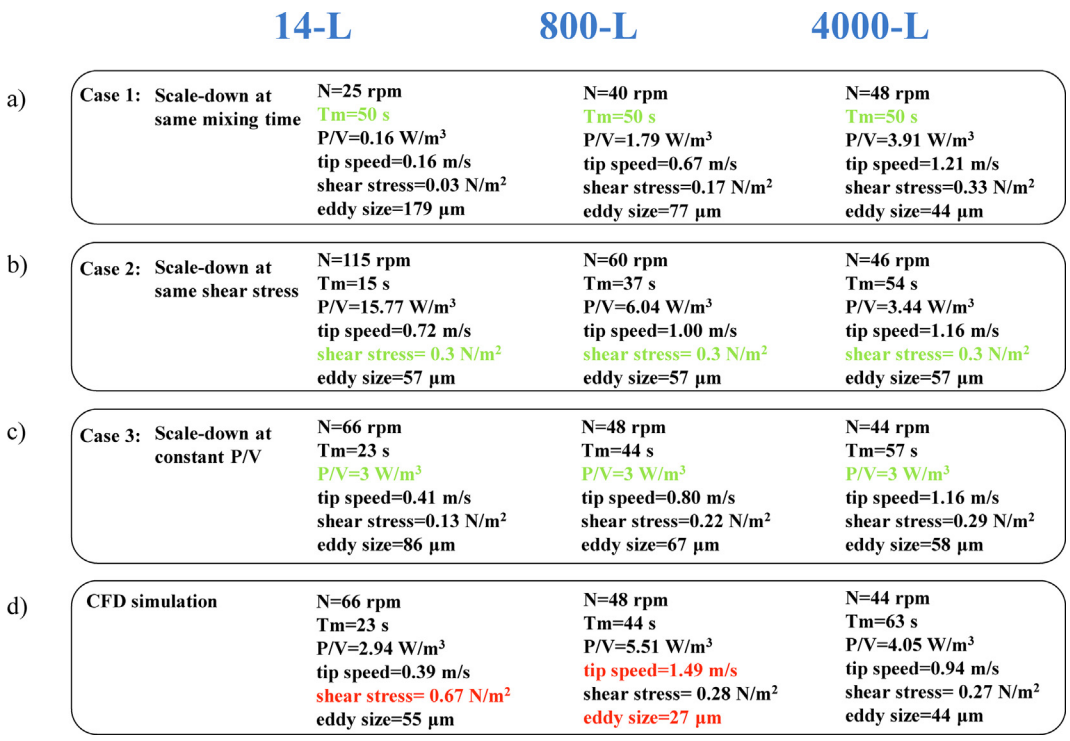

Fig. 2. Comparison of the calculation results (a, b, c) for three scale-down strategies with CFD simulation results of Case 3 (d). Texts in red highlight the most significant difference between (c) and (d). (For interpretation of the references to color in this figure legend, the reader is referred to the web version of this article.)

3.4. CFD simulation

We next used CFD simulation to further evaluate the scale-down strategy (equivalent *P/V*) identified in the previous section, since it is able to provide us with more details about hydrodynamic environments inside the bioreactors.

We set *P/V* value to 3 W/m^3, and then hence calculated the stirring speeds to be 66 rpm, 48 rpm and 45 rpm for 14-L, 800-L and 4000-L bioreactors, respectively. By simulation, we found the mixing times (23.4 s, 44.5 s and 63.7 s) (as shown in Fig. 3) were very close to the values (23 s, 44 s and 57 s) in Case 3 by calculation using Eqs. (14)–(16).

Next, we simulated the flow velocity fields and obtained the whole-tank velocity profiles of three bioreactors by setting the impeller rotational speeds to 66 rpm, 48 rpm and 44 rpm for 14-L, 800-L and 4000-L bioreactors, respectively (Fig. 4a). The maximal flow velocities by simulation for 14-L and 4000-L bioreactors (0.389 m/s and 0.936 m/s) are very close to calculated results in Case 3 (0.41 m/s and 1.16 m/s), while there is 1.86-fold variation for the 800-L bioreactor (1.49 m/s by simulation vs. 0.8 m/s by calculation). Such discrepancy may result from asymmetric design of the impeller location in the tank, which leads to higher mixing efficiency between impeller and baffle. In spite of this, the maximal flow velocities at the edge of paddles for three bioreactors are all within the acceptable range (<2 m/s) [32].

Shear stress is mainly caused by the relative motion of paddles, fluid and wall of tank, which is also a highly concerned parameter in fermentation process since it directly relates to damage of cells in a stirred-tank bioreactor. Through simulation, we obtained the whole-tank shear stress profiles for three bioreactors by setting impeller rotational speeds 66 rpm, 48 rpm and 44 rpm, respectively. As shown in Fig. 4b, the shear stress has very sharp gradient in each reactor near impeller paddles or the wall, but decreases quickly for more than a magnitude towards the fluid side. Shear stress values by simulation are similar to the previous calculated results for 800-L and 4000-L bioreactors (0.219 N/m^2 and 0.288 N/m^2), but the shear stress is unexpected high stress for 14-L bioreactor by simulation (0.666 N/m^2), as compared to the value by calculation (0.132 N/m^2). This implies that hydrodynamic environment in a tank is quite complicated and highlights the importance of CFD simulation.

Mechanical energy generated by stirring leads to formation of eddies in the fluid. Eddies carrying kinetic energy can also damage cells if the cell size is larger than the smallest eddy (for cells in suspension). We obtained eddy size profiles by CFD simulation with the inputting impeller rotational speeds 66 rpm, 48 rpm and 44 rpm for 14-L, 800-L and 4000-L bioreactors, respectively (Fig. 4c). In general, higher stirring speed results in smaller eddy in a bioreactor. The eddy size profiles are symmetrical for two symmetrical tanks (14-L and 4000-L bioreactors), with the smallest sizes 54.6 μm and 44.0 μm, which are comparable to the values 88.6 μm and 57.7 μm by calculation in Section 3.3. By contrast, the smallest eddy in the asymmetric 800-L bioreactor has the size 26.7 μm in simulation, which is significantly away from the calculated value (67 μm). Such eddy size is close to the threshold (20 μm) [25], under which cells in the bioreactor will be damaged.

Finally, we obtained torsional moment (*M*) values 0.00434, 0.548 and 2.58 (N·m), by inputting impeller rotational speeds 66 rpm, 48 rpm and 44 rpm in simulation for 14-L, 800-L and 4000-L bioreactors, respectively. Using the Eq. (17) below, we calculated the *P*/V values to be 2.94, 5.51 and 4.05 W/m^3 for three bioreactors, respectively. These values are different from the constant *P/V* value we initially set (3 W/m^3), but are within acceptable range [33–35].

$$P/V = 2\pi NM/V \tag{17}$$

where *M* is torsional moment (N·m).

Important hydrodynamic parameters of three bioreactors obtained by calculation and CFD simulation are summarized in Fig. 2c and d, in which we also highlight the parameters of signif-

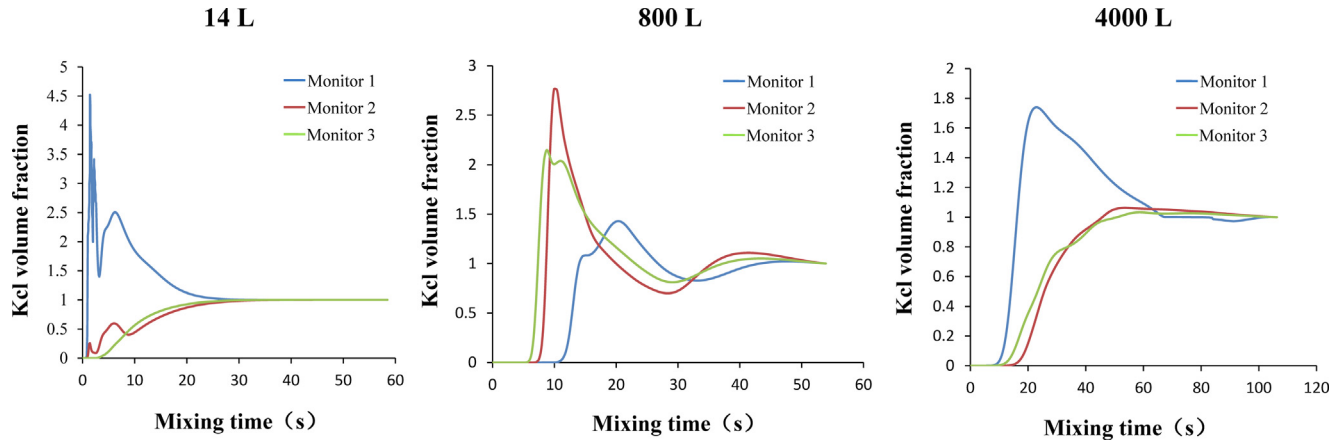

Fig. 3. Simulation of mixing time in 14-L, 800-L and 4000-L bioreactors, with input impeller rotational speeds 66 rpm, 48 rpm and 44 rpm, respectively. Three colors represent monitoring at different locations in bioreactors.

icant difference between two approaches. The values from CFD simulation are more reliable, since this method is based on accurate models. In general, parameters from these two approaches are close and within in appropriate acceptable ranges for a cell culture process, which proves that the scale-down strategy by setting equivalent *P/V* value is feasible.

3.5. k_La

Since the stirring speeds are fixed at constant *P/V* value (3 W/m^3), we adjusted k_La to 54, 49.6 and 46.8 h^{-1} for three bioreactors by modifying the aeration rates. Under this condition, gas transfer is no longer a limiting factor.

3.6. Evaluation the performance of the scale-down model during FMD vaccine production

The scale-down strategy (*P/V* = 3 W/m^3) characterized in previous sections was finally applied to the manufacture of FMD vaccine in14-L, 800-L and 4000-L bioreactors. Cell density, viability, metabolites, and product quality attributes (virus titer, 146 s and total protein) were quantified to evaluate this scale-down strategy.

As described in the section of materials and methods, BHK-21 cells were inoculated with initially 0.5×10^6 viable cells/mL into 14-L, 800-L and 4000-L bioreactors and grown for 48 h. FMD virus was then inoculated after changing media into virus culture media and finally harvested after12 h. In general, three bioreactors behaved very similarly in regard to viable cell density and cell viability in during the whole fermentation process, general. Viabilities were stable (>96.5%) and cell densities increased steadily up to over 3×10^6/mL in the first 48 h for all three bioreactors. Both viabilities and cell densities dropped sharply after 48 h, after inoculation of the virus. We also quantified cellular metabolites (glucose, glutamine, lactate and ammonia) and osmotic pressure during FMD virus production in three different bioreactors, and they also behaved similarly in general (Fig. 5b–f), which once again supports the robustness of our scale-down strategy.

Furthermore, we established a PLS batches model based on the process off-line sampling data from manufacture scale of 4000-L. This model contains four components which can be explained as >98% of process variance, as shown in Fig. 6. Solid lines represent the evolution of the loading plots for three 14-L batches and three 800-L batches over the whole culture time. As we can see, most score points of the six batches are located within the ±3σ limits of the 4000-L model, which proves the similarity of culture process in three bioreactors.

146 s is the main immunogenic of FMD virus, which manifests the total virus number. The amount of infective virus (virus titer) in cell culture broth is assessed via the $TCID_{50}$ assay as an efficacy indicator. Total protein per gram 146 s is a purity indicator, which is relevant to heterogenic protein content leading to harmful reactions. We measured these three parameters for 14-L, 800-L and 1400-L bioreactors, representing product quality attributes. As show in Table 2, the 146 s concentrations achieve 3 μg/mL in 14-L and 4000-L bioreactors, while virus produced by 800-L bioreactor is slightly less ($p > 0.05$ by *T*-test). As for virus titer, $TCID_{50}$ values are close for 14-L and 4000-L bioreactors (7.65 and 7.68 respectively), a little bit higher than that for 800-L scale. Total protein concentration is related to antigenic titer and protein of impurity. We selected total protein per gram 146 s as the quality attribute to characterize virus purity, a key parameter which impacts downstream purification and determines incidence rate of adverse events of vaccine. The data in Table 2 indicates that protein per gram 146 s at three scales are also comparable.

Finally, we applied DOE in scale-down model using QbD principle [36]. Four critical process parameters (CPPs) were found, and the operation parameters of CPPs were adjusted. The control space was then applied in manufacturing scale. Three hundred manufacturing-scale production batches were collected in four years and defect rates were obtained by statistical analysis. As shown in Table 3, the defect rates of all critical quality attributes significantly decreased after optimization by QbD, and the global defect rate decreased from 18.3% to 1.67%.

4. Discussion

In the previous study, we established a scale-up model in which the productivity and product quality reached the releasing specification. However, stability of the product quality varied batch by batch. Therefore, we intended to develop a scale-down model, which could be used for further process optimization in an economic way. We first selected equivalent mixing time, equivalent shear stress and equivalent *P*/*V* as the three candidates to develop the scale-down model for FMD inactivated vaccine production by BHK-21 cells. Key hydrodynamic parameters were calculated and compared for 14-L, 800-L and 4000-L bioreactors, and finally we chose equivalent *P/V* as the scale-down strategy, since in this case no significant variations were observed for these hydrodynamic parameters among three different bioreactors. Next, we used CFD simulation to study the details of hydrodynamic environment in three bioreactors. In general, except for the parameters impacted

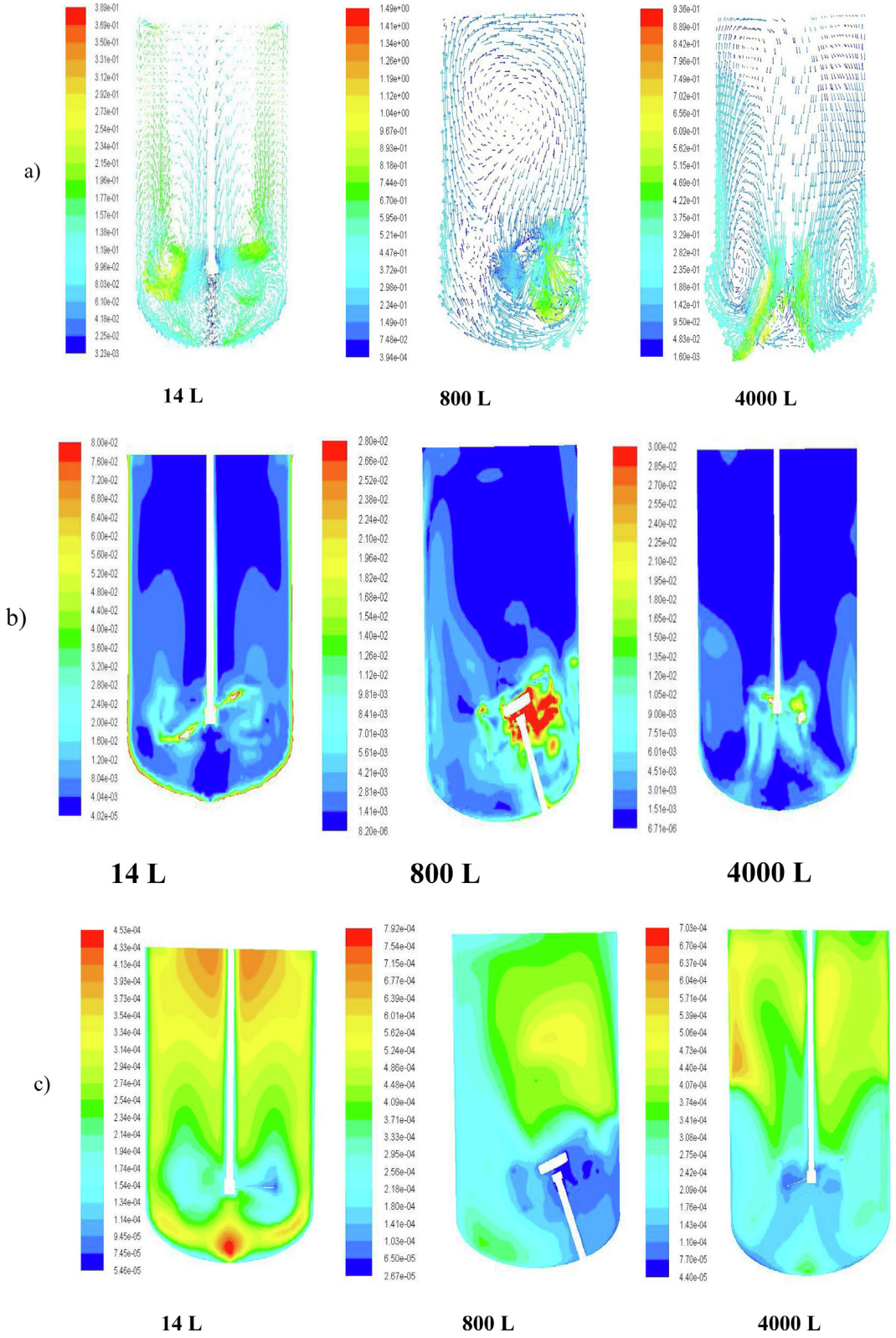

Fig. 4. Simulated velocity (a), shear stress (b) and eddy size (c) profiles for 14-L, 800-L and 4000-L bioreactors, with input impeller rotational speeds 66 rpm, 48 rpm and 44 rpm, respectively. Color gradient represents velocity magnitude, with red symbolizing the highest velocity and dark blue symbolizing the lowest velocity. (For interpretation of the references to color in this figure legend, the reader is referred to the web version of this article.)

by the asymmetric stirring of the 800-L bioreactor, hydrodynamic parameters obtained from CFD simulation were close to the results by calculation, which proves reliability of our scale-down strategy. We also tuned k_La to similar values by adjusting aeration rates for three bioreactors, which eliminated the issue caused by gas transfer, and hence established the scale-down model. Compared to

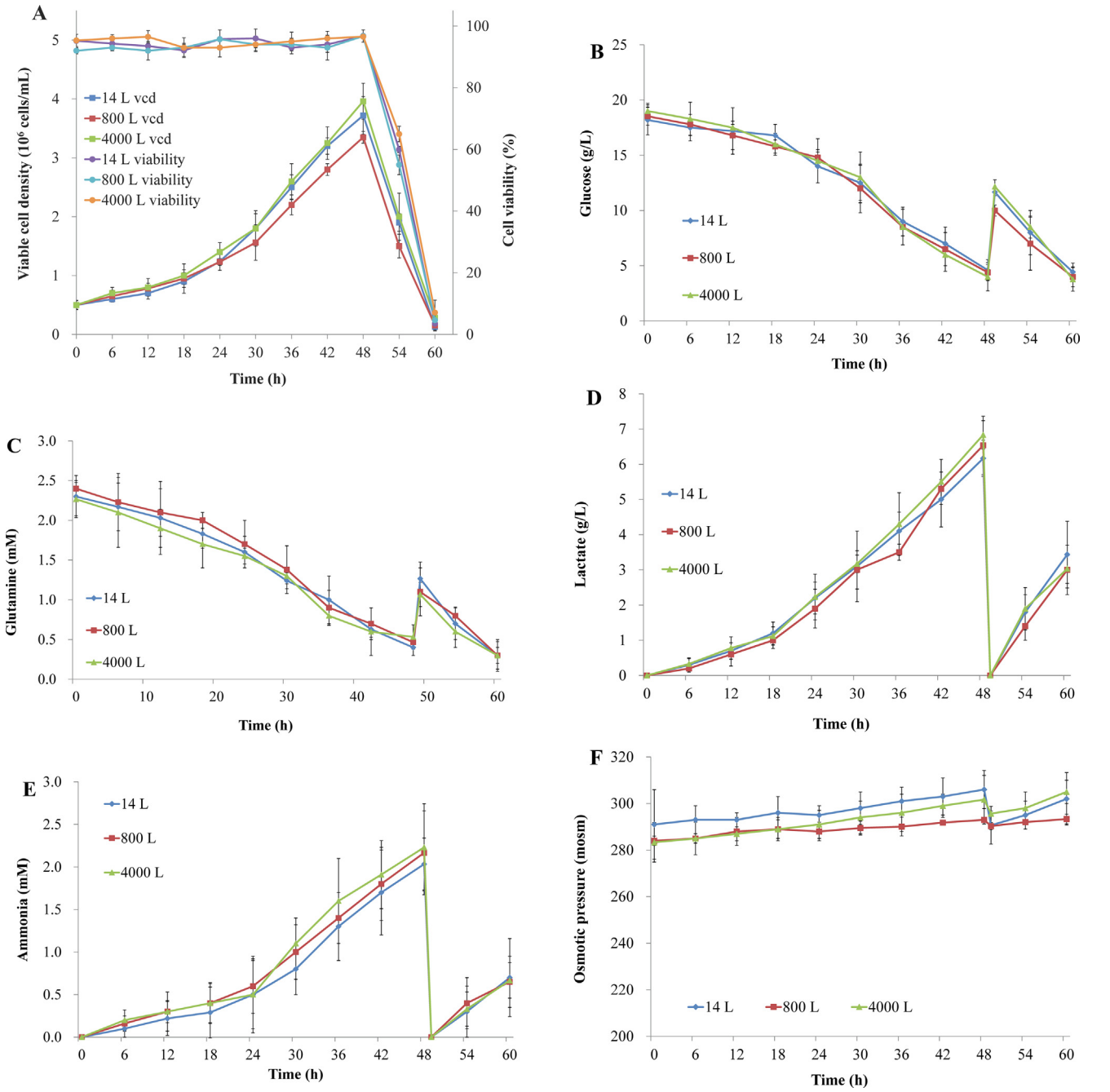

Fig. 5. Comparison of viable cell density and viability (a), glucose (b), glutamine (c), lactate (d), ammonia (e) and osmotic pressure (f) among14-L (n = 3), 800-L (n = 3) and 4000-L (n = 3) bioreactors.

other methods of building scale-down models [16–19], our strategy developed in this study is much simpler and cost saving, since only calculation of hydrodynamic parameters is needed. However, this strategy still needs further refinements, such as integration of gas–liquid flows into CFD.

We evaluated this scale-down model by applying it to FMD vaccine production. We monitored viable cell density, viability, metabolites and osmotic pressure during the fermentation process, which indicates all three bioreactors behaved similarly (Fig. 5). We next established a PLS batches model to further validate the comparability of process performance at different cultivation scales, showing most score points of the validation batches of 14-L and 800-L bioreactors were located within ±3σ limits of 4000-L batch model. We measured three quality attributes (146 s, $TCID_{50}$ and total protein per gram 146 s), with values also very close among three different bioreactors.

It should be noted that the 800-L bioreactor behaved slightly differently, compared to the other two bioreactors, probably due to its unsymmetrical stirring system. The smallest eddy size (26.7 μm) in 800-L bioreactor obtained from CFD simulation is close to cell diameter (20 μm), which potentially triggered cell damage. This issue may also result in the observed lower cell density in 800-L bioreactor at time of infection, which further caused the less amount of 146 s and lower $TCID_{50}$ value at harvesting time, although not significant. Despite of this, most hydrodynamic parameters and quality attributes during the vaccine production

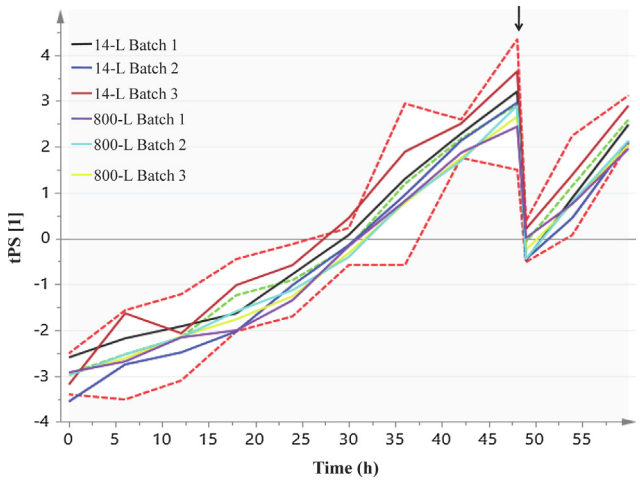

Fig. 6. Process validation using PLS batches model. Two red dashed lines indicate ±3σ limits of 4000-L batches model (n = 3) and the green dashed line represents means. Each of the solid lines stands for score evolution in a cultivation batch for 14-L (n = 3) and 800-L (n = 3) bioreactors. Black arrow indicates time of infection. (For interpretation of the references to color in this figure legend, the reader is referred to the web version of this article.)

Table 2
146 s titer, virus titer and total protein per gram of 146 s for 14-L, 800-L and 4000-L bioreactors by applying the chosen scale-down strategy (constant *P*/*V*). Values represent means of three replicates.

	14-L	800-L	4000-L
146 s (μg/mL)	3.03 ± 0.43	2.47 ± 0.18	3.13 ± 0.53
Virus titer (log $TCID_{50}$/mL)	7.65 ± 0.17	7.53 ± 0.14	7.68 ± 0.13
Total protein/146 s	438 ± 107	393 ± 33.6	423 ± 119

Table 3
Defect rates of critical quality attributes before and after optimization by applying QbD strategy in the scale-down model.

Critical quality attribute	Before optimization	After optimization
$TCID_{50}$	3.33%	0%
Antigenic titer	13.3%	1.33%
Total protein	9.33%	0.67%
All	18.3%	1.67%

are very similar among three different bioreactors, which proves we have successfully established a scale-down model representing the large-scale manufacturing process for FMD inactivated vaccine. Finally, we applied DOE in the scale-down model according to QbD. The global defect rate of 4000-L manufacture product was significantly reduced from 18.3% to 1.67%.

5. Conclusion

In this study, we identified equivalent *P*/*V* as the scale-down strategy to represent large-scale process for FMD inactivated vaccine production by BHK-21 cells, through calculations using theory of hydrodynamics and CFD simulation. Similar performance of three bioreactors with different scales proves robustness of this scale-down strategy. Such approach could also be transferred to other manufacturing processes, such as microbial fermentation by *E. coli* or yeast.

Declaration of Competing Interest

The authors declare that they have no known competing financial interests or personal relationships that could have appeared to influence the work reported in this paper.

Acknowledgments

This work was supported by the National Natural Science Foundation of China (31570034), the National First-class Discipline Program of Light Industry Technology and Engineering (LITE2018-24), the Opening Project of the Key Laboratory of Industrial Biotechnology, Ministry of Education (KLIB-KF201802), the Collaborative Innovation Center of Jiangsu Modern Industrial Fermentation, the 111 Project (111-2-06), the Priority Academic Program Development of Jiangsu Higher Education Institutions, and the Achievements Transformation Project of Gansu Province (17ZD4CA010), Research Innovation Program for College Graduates of Jiangsu Province (KYLX16_0807).

References

[1] Grubman MJ, Baxt B. Foot-and-mouth disease. Clin Microbiol Rev 2004;17:465–93.
[2] Acharya R, Fry E, Stuart D, Fox G, Rowlands D, Brown F. The three-dimensional structure of foot-and-mouth disease virus at 2.9 Å resolution. Nature 1989;337:709.
[3] Alexandersen S, Zhang Z, Donaldson AI, Garland AJ. The pathogenesis and diagnosis of foot-and-mouth disease. J Comp Pathol 2003;129:1–36.
[4] De Bravo RC, Dekker A, Eblé PL, De Jong MC. Vaccination of cattle only is sufficient to stop FMDV transmission in mixed populations of sheep and cattle. Epidemiol Infect 2015;143:2279–86.
[5] Barteling SJ. Development and performance of inactivated vaccines against foot and mouth disease. Rev Sci Tech 2002;21:577–88.
[6] Vallee H, Carre H, Rinjard P. On immunisation against foot-and-mouth disease. Rech Med Vet 1925;101:297–9.
[7] Sanford KK, Earle WR, Likely GD. The growth in vitro of single isolated tissue cells. J Natl Cancer Inst 1948;9:229–46.
[8] Lombard M, Pastoret PP, Moulin AM. A brief history of vaccines and vaccination. Rev Sci Tech 2007;26:29–48.
[9] Mowat G, Chapman W. Growth of foot-and-mouth disease virus in a fibroblastic cell line derived from hamster kidneys. Nature 1962;194:253.
[10] Capstick P, Telling R, Chapman W, Stewart DL. Growth of a cloned strain of hamster kidney cells in suspended cultures and their susceptibility to the virus of foot-and-mouth disease. Nature 1962;195:1163.
[11] Nienow AW, Scott WH, Hewitt CJ, Thomas CR, Lewis G, Amanullah A, et al. Scale-down studies for assessing the impact of different stress parameters on growth and product quality during animal cell culture. Chem Eng Res Des 2013;91:2265–74.
[12] Xing Z, Kenty BM, Li ZJ, Lee SS. Scale-up analysis for a CHO cell culture process in large-scale bioreactors. Biotechnol Bioeng 2009;103:733–46.
[13] Marks DM. Equipment design considerations for large scale cell culture. Cytotechnology 2003;42:21–33.
[14] Nienow AW. Reactor engineering in large scale animal cell culture. Cytotechnology 2006;50:9–33.
[15] Yang JD, Lu C, Stasny B, Henley J, Guinto W, Gonzalez C, et al. Fed-batch bioreactor process scale-up from 3-L to 2,500-L scale for monoclonal antibody production from cell culture. Biotechnol Bioeng 2007;98:141–54.
[16] Noorman H. An industrial perspective on bioreactor scale-down: what we can learn from combined large-scale bioprocess and model fluid studies. Biotechnol J 2011;6:934–43.
[17] Ahuja S, Jain S, Ram K. Application of multivariate analysis and mass transfer principles for refinement of a 3-L bioreactor scale-down model–when shake flasks mimic 15,000-L bioreactors better. Biotechnol Prog 2015;31:1370–80.
[18] Delvigne F, Takors R, Mudde R, van Gulik W, Noorman H. Bioprocess scale-up/down as integrative enabling technology: from fluid mechanics to systems biology and beyond. Microb Biotechnol 2017;10:1267–74.
[19] Haringa C, Tang W, Wang G, Deshmukh AT, Winden WAV, Chu J, et al. Computational fluid dynamics simulation of an industrial P. chrysogenum fermentation with a coupled 9-pool metabolic model: towards rational scale-down and design optimization. Chem Eng Sci 2017;175. S0009250917305742.
[20] Garcia-Ochoa F, Gomez E. Bioreactor scale-up and oxygen transfer rate in microbial processes: an overview. Biotechnol Adv 2009;27:153–76.
[21] Farrell P, Sun J, Champagne P-P, Lau H, Gao M, Sun H, et al. The use of dissolved oxygen-controlled, fed-batch aerobic cultivation for recombinant protein subunit vaccine manufacturing. Vaccine 2015;33:6752–6.
[22] McCoy R, Ward S, Hoare M. Sub-population analysis of human cancer vaccine cells-ultra scale-down characterization of response to shear. Biotechnol Bioeng 2010;106:584–97.
[23] Harris C, Roekaerts D, Rosendal F, Buitendijk F, Daskopoulos P, Vreenegoor A, et al. Computational fluid dynamics for chemical reactor engineering. Chem Eng Sci 1996;51:1569–94.
[24] Brucato A, Ciofalo M, Grisafi F, Tocco R. On the simulation of stirred tank reactors via computational fluid dynamics. Chem Eng Sci 2000;55:291–302.
[25] Hinze JO, Uberoi MS. Turbulence. New York: McGraw-Hill; 1975.
[26] Riet KVT, Tramper J. Basic bioreactor design. Florida: CRC Press; 1991.
[27] Pope SB. Turbulent flows. Cambridge: Cambridge University Press; 2000.

[28] Rao G. Dynamic measurement of the volumetric oxygen transfer coefficient in fermentation systems. Biotechnol Bioeng 2009;104:841–53.
[29] Rimmelzwaan GF, Baars M, Claas EC, Osterhaus AD. Comparison of RNA hybridization, hemagglutination assay, titration of infectious virus and immunofluorescence as methods for monitoring influenza virus replication in vitro. J Virol Methods 1998;74:57–66.
[30] Fayet MT, Fargeaud D, Louisot P, Stellmann C, Roumiantzeff M. Physical chemical measurement of 140S particles of the foot-and-mouth disease virus. Ann Inst Pasteur (Paris) 1971:107–18.
[31] Wold S, Kettaneh N, MacGregor J, Dunn K. Batch processes: modelling, analysis and control. Amsterdam, The Netherlands: Elsevier; 2008.
[32] Chalmers J. Animal cell culture, effects of agitation and aeration on cell adaptation. In: Spier R, Griffins JB, Scragg AH, editors. Encyclopedia of cell technology. New York: Wiley; 2000. p. 41–51.
[33] Sieck JB, Cordes T, Budach WE, Rhiel MH, Suemeghy Z, Leist C, et al. Development of a scale-down model of hydrodynamic stress to study the performance of an industrial CHO cell line under simulated production scale bioreactor conditions. J Biotechnol 2013;164:41–9.
[34] Lee TS. A methodological approach to scaling up fermentation and primary recovery processes to the manufacturing scale for vaccine production. Vaccine 2009;27:6439–43.
[35] Thomassen YE, van't Oever AG, Vinke M, Spiekstra A, Wijffels RH, van der Pol LA, et al. Scale-down of the inactivated polio vaccine production process. Biotechnol Bioeng 2013;110:1354–65.
[36] Li X, Liu X, Wang R, An F, Nie J, Zhang Y, et al. Quality by design-driven process development of cell culture in bioreactor for the production of foot-and-mouth veterinary vaccine. J Pharm Sci 2019;108:2288–95.